Hindawi Publishing Corporation
Journal of Nanomaterials
Volume 2011, Article ID 582764, 6 pages
doi:10.1155/2011/582764

*Research Article*

# Rapid Hydrothermal Synthesis of Zinc Oxide Nanowires by Annealing Methods on Seed Layers

**Jang Bo Shim,[1] Hyuk Chang,[2] and Sung-O Kim[3]**

[1] *Device Materials Research Center, Korea Research Institute of Chemical Technology, P.O Box 107, Sinseongno 19, Yuseong-gu, Daejeon 305-600, Republic of Korea*
[2] *Energy Laboratory, Samsung Advanced Institute of Technology, Samsung Electronics, Suwon 446-712, Republic of Korea*
[3] *Holcombe Department of Electrical and Computer Engineering, Center for Optical Materials Science and Engineering Technologies, Clemson University, Clemson, SC 29634, USA*

Correspondence should be addressed to Sung-O Kim, sok@clemson.edu

Received 27 September 2010; Revised 17 December 2010; Accepted 7 March 2011

Academic Editor: Cui ChunXiang



Well-aligned zinc oxide (ZnO) nanowire arrays were successfully synthesized on a glass substrate using the rapid microwave heating process. The ZnO seed layers were produced by spinning the precursor solutions onto the substrate. Among coatings, the ZnO seed layers were annealed at 100°C for 5 minutes to ensure particle adhesion to the glass surface in air, nitrogen, and vacuum atmospheres. The annealing treatment of the ZnO seed layer was most important for achieving the high quality of ZnO nanowire arrays as ZnO seed nanoparticles of larger than 30 nm in diameter evolve into ZnO nanowire arrays. Transmission electron microscopy analysis revealed a single-crystalline lattice of the ZnO nanowires. Because of their low power (140 W), low operating temperatures (90°C), easy fabrication (variable microwave sintering system), and low cost (90% cost reduction compared with gas condensation methods), high quality ZnO nanowires created with the rapid microwave heating process show great promise for use in flexible solar cells and flexible display devices.

## 1. Introduction

ZnO, a wide-band gapsemiconductor (Eg = 3.37 eV) [1], has been synthesized to nanowire via various methods, such as chemical vapor deposition [2–4], vapor-liquid-solid growth [5, 6], pulsed laser ablation techniques [7], and solution chemistry [8–11] in constructing nanoscale electronic and optoelectronic devices. Vapor-based synthesis produces high-crystalline and high-aspect-ratio ZnO nanowires with lengths of several microns, owing to the high synthesis temperatures (450 to 900°C) and high vacuum ambient. However, it has a limit for the large scaling of the substrate and flexible electronic device integration as the hydrothermal methods for synthesizing ZnO nanowires operate at much lower temperatures (below 100°C) and atmospheric pressure. Nevertheless, this hydrothermal method has been used successfully to demonstrate the fabrication of large arrays of vertical ZnO nanowires on glass, 4-inch diameter Si wafers [12], and plastic substrates [13].

A thorough investigation of hydrothermal ZnO nanowire synthesis revealed that the time necessary for this synthesis ranged from several hours to several days [12, 14–17]. To solve this problem, Jung et al. recently investigated tip sonication as a quick method for the aligned ZnO nanowire synthesis [18], and Hu et al. studied the possibility of using microwave heating to rapidly synthesize micron-sized ZnO particles [19]. Microwave heating has also been investigated for rapid synthesis of ZnO nanowire by Unalan et al. [20]. Most previous research in this area has focused on the rapid synthesis of ZnO nanowire and postannealing treatment of ZnO nanowire in air, $O_2$, or vacuum ambient. However, vertical well-aligned ZnO nanowire arrays and annealing treatment for ZnO seed layers on glass substrate have yet to be achieved. Consequently, this study annealed in different

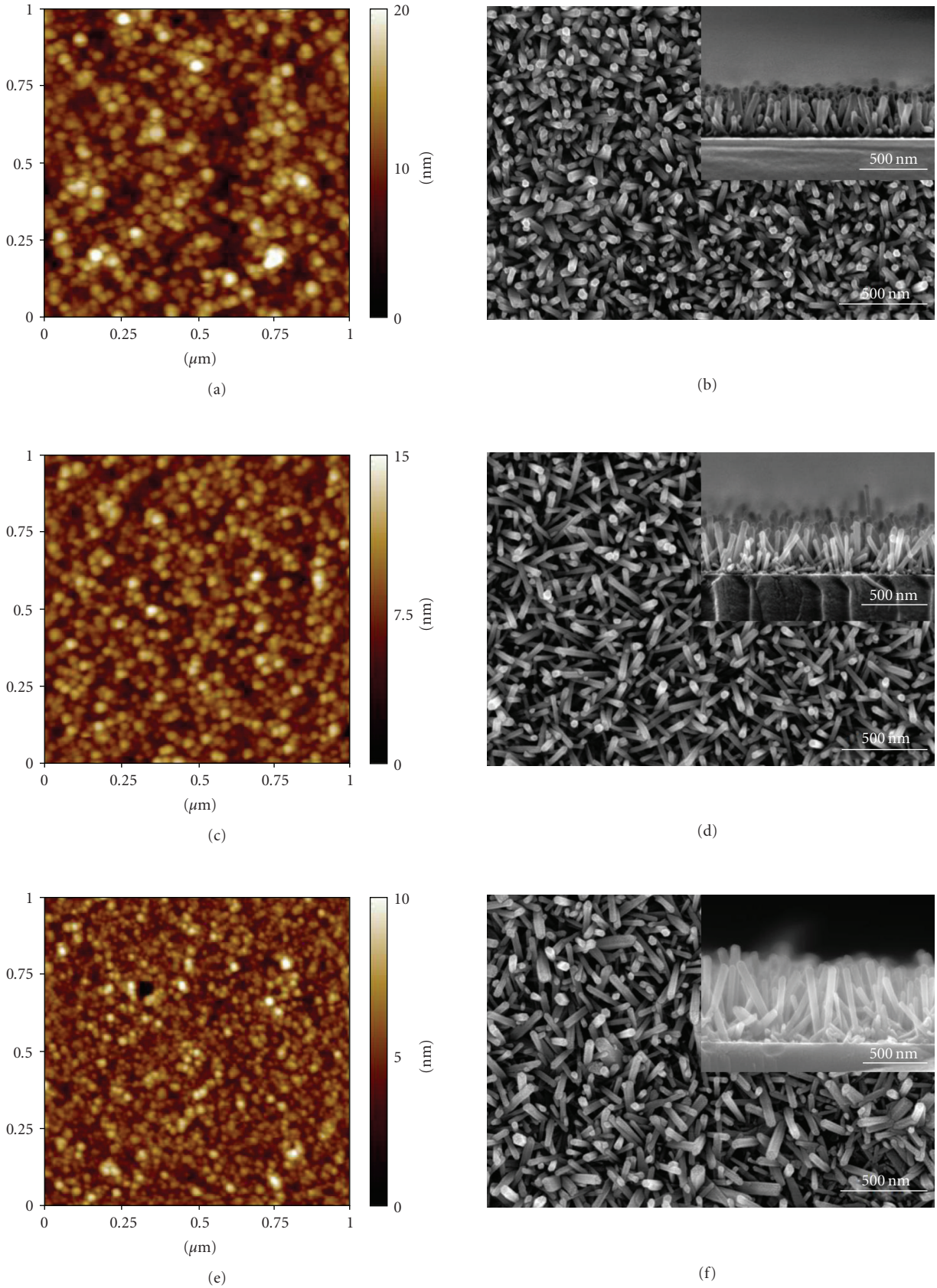


Figure 1: AFM images of the ZnO seed layers with annealing (a) in air, (c) in $N_2$, and (e) in a vacuum; SEM micrographs of the ZnO nanowire arrays under three different seed layer annealing conditions: (b) air, (d) $N_2$, and (f) vacuum. The insets show the cross-sectional view of the ZnO nanowire arrays.

conditions for ZnO seed layer is essential for obtaining high-quality and well-aligned ZnO nanowire arrays.

## 2. Experimental Details

In this study, we report on the optimal synthesis conditions for preparing well-aligned ZnO nanowire arrays using the rapid microwave heating process. These well-aligned ZnO nanowires were grown using a two-step process: (a) preparation of the seed layer and (b) growth of the nanowire arrays. In the first step, coating solutions (20 mM) were prepared by a zinc acetate dihydrate (98%, Aldrich) and 1-propanol (spectroscopic grade). The ZnO seed layers were produced by spinning the precursor solutions on a glass substrate. Among coatings, the ZnO seed layers were annealed at 100°C for 5 minutes to ensure particle adhesion to the glass surface in air, nitrogen ($N_2$), and vacuum atmospheres. A uniform seed layer was obtained after three layers of spin coating. ZnO nanowires were then grown by dipping the substrates in a mixture of equimolar 25 mM zinc nitrate hexahydrate ($Zn(NO_3)_2 \cdot 6H_2O$, Sigma Aldrich) and hexamethylenetetramine (HMTA, Sigma Aldrich) solution in deionized (DI) water and heating with a variable microwave sintering system (2.45 GHz) at 140 W power setting and atmospheric pressure as the optimal condition. Microwave heating was performed for 10 to 30 min; a revolving turntable within the sintering system ensured a homogeneous heating of the solution. The obtained ZnO nanowire arrays on the glass substrate were removed from the solution, rinsed with DI water, and dried.

The surface morphology of the ZnO seed layer was observed by atomic force microscopy (AFM). The morphology and size of the ZnO nanowires were investigated by field emission scanning electron microscopy (FESEM) (Hitachi S-4800S, operated at 15 kV), and the crystallinity of the ZnO nanowires was investigated using high-resolution transmission electron microscopy (HRTEM) (Hitachi 9500, operated at 300 kV). HRTEM specimens were prepared by scraping wires from the substrates, followed by dispersion in ethanol and then drop cast onto the copper grids. The crystal structure of the ZnO nanowires was observed using X-ray diffraction (XRD) (Scintag XDS-2000 diffractometer) with CuK$\alpha$ radiation. The optical characteristics of the as-grown nanowires were investigated using photoluminescence (PL) measurements. The PL measurements were performed at room temperature with the 325 nm line of a Xenon laser. The X-ray photoelectron spectroscopy (XPS) was measured by using a Kratos AXIS 165 instrument with monochromated AlK$\alpha$ radiation.

## 3. Results and Discussion

Figure 1 shows the AFM images of the ZnO seed layers and the SEM images of the ZnO nanowire arrays in the optimal conditions (140 W, 2.45 GHz, and 30 minutes). At the annealing temperature of 100°C, the seed layer exhibits no grain forms, whereas, at the annealing temperature of 300°C, the seed layer contains fine grains [21]. As shown in Figures 1(a), 1(c), and 1(e), uniform ZnO nanoparticles adhering to the glass substrate were observed, which serve as the nucleation centers. The initial stage for the ZnO seed layer is a critical component in obtaining the high quality of uniform ZnO nanowire arrays. The size distribution of the ZnO nanoparticles at air annealing conditions is more uniform and narrower compared to nitrogen and vacuum annealing conditions. The dispersion and agglomeration of ZnO nanoparticles on the glass substrate are not identical due to the different annealing conditions. The higher uniformity of seed layer on air annealing condition, in turn, leads to the growth of higher-quality ZnO nanowire arrays. The density of ZnO nanoparticles annealed in air, in $N_2$, and in a vacuum calculated from Figures 1(a), 1(c), and 1(e) is 664 $\mu m^{-2}$, 840 $\mu m^{-2}$, and 1160 $\mu m^{-2}$, respectively. Though the density of the ZnO nanowire arrays on the ZnO seed layer annealed with the vacuum is approximately 220 $\mu m^{-2}$, as calculated from the SEM image, the density of ZnO nanoparticles calculated from the AFM image is approximately 1160 $\mu m^{-2}$. This discrepancy indicates that the ZnO seed nanoparticles of larger than approximately 30 nm diameter can evolve into ZnO nanowire arrays. In air annealing conditions, the average diameter of ZnO nanoparticles increased, which thus enhanced the alignment of the nanowire arrays. If the ZnO nanowires have a broad size distribution, this interaction will cause the small nanowires under asymmetric force to bend easily, degrading the nanowire alignment [22]. Figures 1(b), 1(d), and 1(f) show the SEM images of top view and cross-sectional view for the ZnO nanowire arrays corresponding to Figures 1(a), 1(c), and 1(e), respectively. These were grown at a fixed temperature 90°C, while the seed layers were annealed at 100°C with air, $N_2$, and vacuum conditions, respectively. The SEM image of the ZnO nanowire arrays on the ZnO seed layer annealed at air clearly shows a high density of vertically grown ZnO nanowire arrays with well-defined hexagonal facets (001). These nanowire arrays have

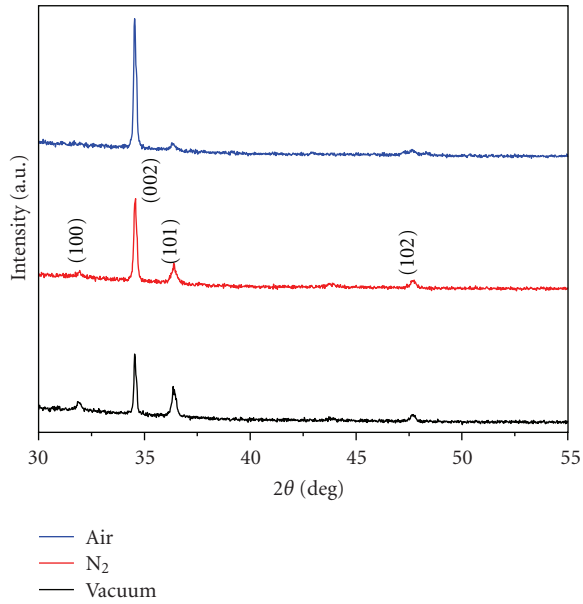


Figure 2: XRD patterns of the ZnO nanowire arrays at three different seed layer annealing conditions: air, $N_2$, and vacuum.

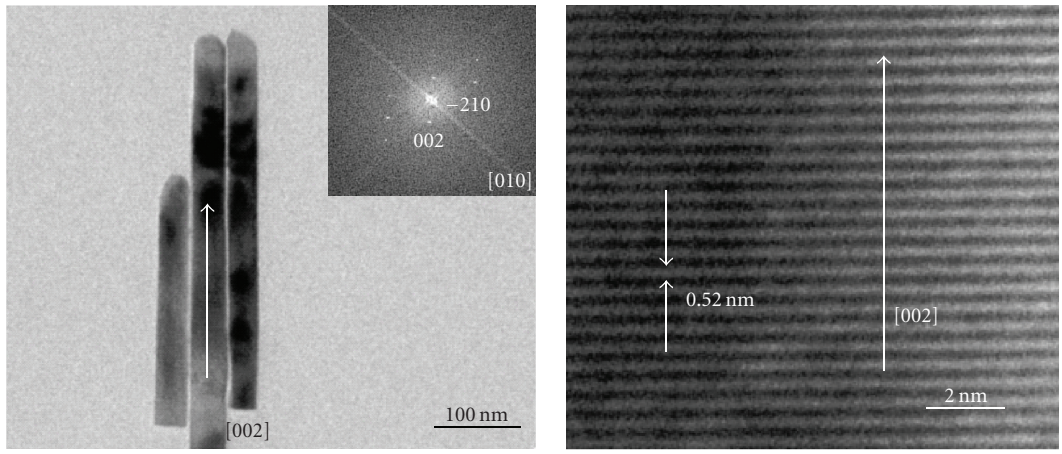


Figure 3: (a) TEM image of the ZnO nanowire arrays on the ZnO seed layer annealed in air; the inset shows the corresponding FFT pattern. (b) HRTEM image of the ZnO nanowire array, in which the lattice spacing is 0.52 nm along the [002] direction.

a narrow size distribution centered of approximately 38 nm in diameter in Figure 1(b). The cross-sectional view (inset of Figure 1(b)) of the ZnO nanowire arrays indicates that the ZnO nanowire arrays grew vertically with identical lengths of 340 nm. The annealing condition of the ZnO seed layer is a key influence on the nucleation of the ZnO nanowire array. Furthermore, the ZnO nanowire arrays on the ZnO seed layer annealed at air are well aligned both vertically and uniformly (Figure 1(b)). The well-defined crystallographic planes of the hexagonal-shaped nanowires can be clearly identified, providing strong evidence that the ZnO nanowire arrays orientate along the c-axis.

Figure 2 shows the XRD patterns of the ZnO nanowire arrays. It did not appear that any other characteristic peaks corresponding to the impurities of the precursors such as zinc nitrate and zinc hydroxide were observed in the XRD patterns. At the ZnO nanowire arrays on the ZnO seed layer annealed in air, a very strong (002) diffraction peak and a very weak (101) peak are observed, indicating a high c-axis orientation of the ZnO nanowire array. In addition, the intensity of the (002) diffraction peak is the strongest, compared to other samples annealed in both $N_2$ and vacuum conditions. This result, in accordance with its SEM image of Figure 1(b), implies its perfect c-axis orientation. However, for the ZnO nanowire arrays on the ZnO seed layer annealed in a vacuum, the (002) diffraction peak weakens while the (100) and (101) peaks slightly increase in strength, indicating its tendency toward random orientation. These conclusions closely match the SEM image of the ZnO nanowire arrays observed in Figure 1(f). The previous XRD investigation of the seed layers annealed at 100°C by Asakuma et al. indicates a nearly amorphous structure which agrees with our result [23]. However, the ZnO nanowire arrays are highly (002) plane-oriented on an amorphous ZnO seed layer. This orientation indicates that the ZnO nanowire arrays prepared by the rapid microwave heating process have preferential orientation along the (002) plane on the seed layer without a certain orientation.

The TEM image and the corresponding fast Fourier transform (FFT) pattern are shown in Figure 3(a). Here, it is clearly evident that individual ZnO nanowire arrays with a diameter of 38 nm grown along the [002] direction possess a single-crystalline wurtzite structure. The high-resolution TEM image in Figure 3(b) also shows that the ZnO nanowire array is structurally uniform. We also see the clear d-spacing of (002) crystal planes, confirming that the ZnO nanowire arrays grown with the rapid microwave heating process are preferentially oriented in the c-axis direction.

The PL spectrum shown in Figure 4 was derived at room temperature. The peak due to the near-bandgap edge emission of the wide-bandgap ZnO is centered at 380 nm. At the ZnO nanowire arrays on the ZnO seed layer annealed in air, the defect-related green emission (565 nm) of the ZnO nanowire arrays is lower than in the $N_2$ and vacuum annealing conditions. The green emission is also known to be a deep-level emission caused by the impurities and structural defects in the crystal (e.g., oxygen vacancies, zinc interstitials) [24]. According to the annealing conditions, the PL peak in the green emission region is gradually enhanced, which is believed to result from oxygen vacancies. Therefore, it is suggested that the ZnO nanowire arrays may reduce the defect density and hence lower the defect-related emission caused by the ZnO seed layer annealed in air conditions. Moreover, the ZnO nanowire arrays on the ZnO seed layer annealed in air have a highly delineated (002) orientation and vertical alignment.

Figure 5 shows XPS spectra of O1s for ZnO nanowire arrays, fitted with Gaussian-Lorentz distribution (70 : 30 ratio). The O1s peak was constructed of subpeaks at 527.2 eV and 528.5 eV, respectively. The peak with low binding energy (527.2 eV) corresponds to $O^{2-}$ on normal wurtzite structure of a ZnO single crystal [25]. Another peak centered at 528.5 eV is attributed to $O^{2-}$ in the oxygen vacancies within the ZnO matrix [26]. The O1s peaks for the ZnO nanowire arrays on the ZnO seed layer annealed at vacuum have a shoulder at higher binding energy as shown in Figure 5(c),

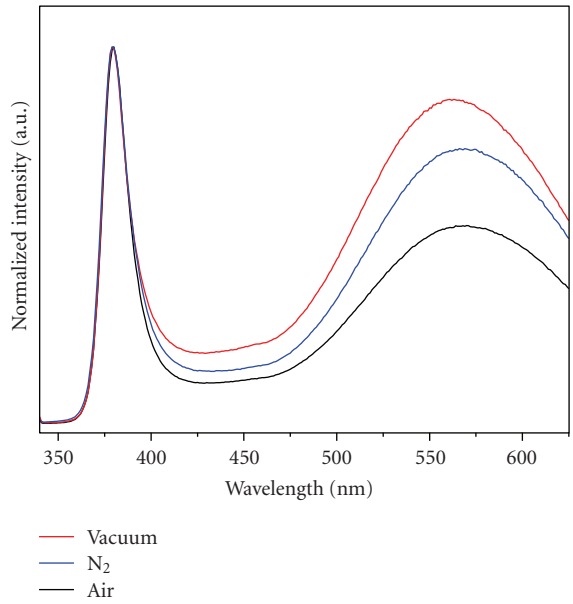


Figure 4: Normalized room temperature PL spectra of the ZnO nanowire arrays using 325 nm line as the excitation source.

which gradually decreases for annealed samples in $N_2$ and in air. From the observation of O1s peaks, it is clear that the oxygen vacancies of the ZnO nanowire arrays decrease with annealing in air conditions. Annealing in $N_2$ and vacuum can cause a deviation from the stoichiometric state, resulting in large oxygen deficiencies [27]. These oxygen deficiencies were decreased by O that was complemented with annealing in air. These results indicate that the stoichiometry and structure of ZnO seed layers annealed in air are superior to those of ZnO layers annealed in both $N_2$ a vacuum. The XPS measurement supports this PL observation. These observations indicate that the ZnO nanowire arrays on the ZnO seed layer annealed at vacuum degrade the nanowire quality, thus creating oxygen vacancies.

## 4. Conclusion

High-quality and well-aligned ZnO nanowire arrays were successfully synthesized on glass substrate by the rapid microwave heating process. We verified that the annealing treatment for ZnO seed layer was very important for achieving the high quality of ZnO nanowire arrays as ZnO seed nanoparticles of larger than 30 nm in diameter evolve into ZnO nanowire arrays. The ZnO nanowire arrays on the ZnO seed layer annealed at air are highly c-axis-oriented and perpendicular to the substrate with high crystalline quality compared with $N_2$ and vacuum annealed ZnO nanowires. The PL measurements show that the ZnO seed layer annealed in air yields low levels of oxygen vacancies in the ZnO nanowire arrays. The high-quality ZnO nanowires created with the rapid microwave heating process show a great promise for use in flexible solar cells, flexible displays, and other flexible devices with low power, low growth temperature, short growth time, easy fabrication, and low cost.

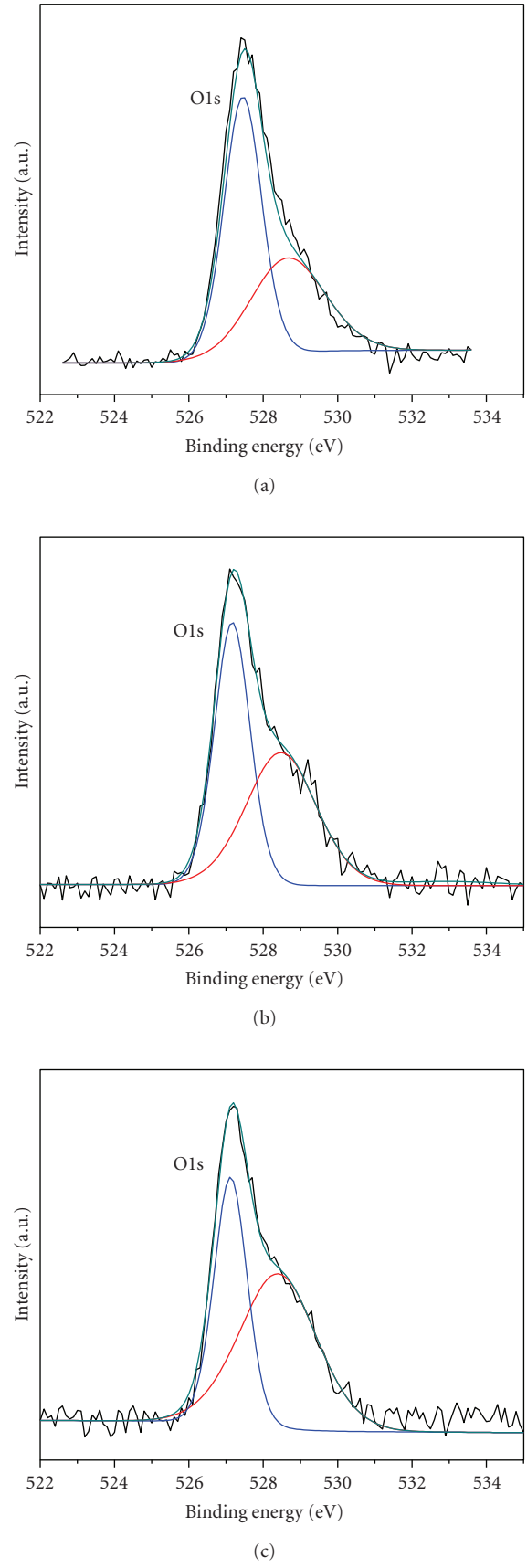


Figure 5: XPS spectra of the ZnO nanowire arrays at three different seed layer annealing conditions: (a) air, (b) $N_2$, and (c) vacuum.

## Acknowledgments

The authors wish to thank Samsung Advanced Institute of Technology in Samsung Electronics and the Center for Optical Materials Science and Engineering Technologies (COMSET) in Clemson University for their financial support. The authors also thank Dr. T. Darroudi, Dr. H. Qian, and Dr. J. S. Hudson of Clemson University Electron Microscope Facility for technical assistance and Dr. J. E. Harriss for the Microstructures Laboratory.

## References

[1] D. C. Reynolds, D. C. Look, B. Jogai et al., "Neutral-donor-bound-exciton complexes in ZnO crystals," *Physical Review B*, vol. 57, no. 19, pp. 12151–12155, 1998.

[2] J. J. Wu and S. C. Liu, "Low-temperature growth of well-aligned ZnO nanorods by chemical vapor deposition," *Advanced Materials*, vol. 14, no. 3, pp. 215–218, 2002.

[3] B. Xiang, P. Wang, X. Zhang et al., "Rational synthesis of p-type zinc oxide nanowire arrays using simple chemical vapor deposition," *Nano Letters*, vol. 7, no. 2, pp. 323–328, 2007.

[4] W. I. Park, G. C. Yi, M. Kim, and S. J. Pennycook, "ZnO nanoneedles grown vertically on Si substrates by non-catalytic vapor-phase epitaxy," *Advanced Materials*, vol. 14, no. 24, pp. 1841–1843, 2002.

[5] X. Wang, J. Song, P. Li et al., "Growth of uniformly aligned ZnO nanowire heterojunction arrays on GaN, AlN, and $Al_{0.5}Ga_{0.5}N$ substrates," *Journal of the American Chemical Society*, vol. 127, no. 21, pp. 7920–7923, 2005.

[6] S. J. Young, L. W. Ji, S. J. Chang et al., "Nanoscale mechanical characteristics of vertical ZnO nanowires grown on ZnO:Ga/glass templates," *Nanotechnology*, vol. 18, no. 22, Article ID 225603, 2007.

[7] YE. Sun, G. M. Fuge, and M. N. R. Ashfold, "Growth of aligned ZnO nanorod arrays by catalyst-free pulsed laser deposition methods," *Chemical Physics Letters*, vol. 396, no. 1–3, pp. 21–26, 2004.

[8] S. Yamabi and H. Imai, "Growth conditions for wurtzite zinc oxide films in aqueous solutions," *Journal of Materials Chemistry*, vol. 12, no. 12, pp. 3773–3778, 2002.

[9] L. Vayssieres, "Growth of arrayed nanorods and nanowires of ZnO from aqueous solutions," *Advanced Materials*, vol. 15, no. 5, pp. 464–466, 2003.

[10] Z. R. Tian, J. A. Voigt, J. Liu et al., "Complex and oriented ZnO nanostructures," *Nature Materials*, vol. 2, no. 12, pp. 821–826, 2003.

[11] L. E. Greene, B. D. Yuhas, M. Law, D. Zitoun, and P. Yang, "Solution-grown zinc oxide nanowires," *Inorganic Chemistry*, vol. 45, no. 19, pp. 7535–7543, 2006.

[12] L. E. Greene, M. Law, J. Goldberger et al., "Low-temperature wafer-scale production of ZnO nanowire arrays," *Angewandte Chemie*, vol. 42, no. 26, pp. 3031–3034, 2003.

[13] J. B. Cui, C. P. Daghlian, U. J. Gibson, R. Püsche, P. Geithner, and L. Ley, "Low-temperature growth and field emission of ZnO nanowire arrays," *Journal of Applied Physics*, vol. 97, no. 4, Article ID 044315, 7 pages, 2005.

[14] L. Vayssieres, K. Keis, S. E. Lindquist, and A. Hagfeldt, "Purpose-built anisotropie metal oxide material: 3D highly oriented microrod array of ZnO," *Journal of Physical Chemistry B*, vol. 105, no. 17, pp. 3350–3352, 2001.

[15] K. Govender, D. S. Boyle, P. O'Brien, D. Binks, D. West, and D. Coleman, "Room-temperature lasing observed from ZnO nanocolumns grown by aqueous solution deposition," *Advanced Materials*, vol. 14, no. 17, pp. 1221–1224, 2002.

[16] X. Ma, H. Zhang, Y. Ji, J. Xu, and D. Yang, "Sequential occurrence of ZnO nanopaticles, nanorods, and nanotips during hydrothermal process in a dilute aqueous solution," *Materials Letters*, vol. 59, no. 27, pp. 3393–3397, 2005.

[17] M. Law, L. E. Greene, J. C. Johnson, R. Saykally, and P. Yang, "Nanowire dye-sensitized solar cells," *Nature Materials*, vol. 4, no. 6, pp. 455–459, 2005.

[18] S. H. Jung, E. Oh, K. H. Lee, W. Park, and S. H. Jeong, "A sonochemical method for fabricating aligned ZnO nanorods," *Advanced Materials*, vol. 19, no. 5, pp. 749–753, 2007.

[19] X. L. Hu, Y. J. Zhu, and S. W. Wang, "Sonochemical and microwave-assisted synthesis of linked single-crystalline ZnO rods," *Materials Chemistry and Physics*, vol. 88, no. 2-3, pp. 421–426, 2004.

[20] H. E. Unalan, P. Hiralal, N. Rupesinghe, S. Dalal, W. I. Milne, and G. A. J. Amaratunga, "Rapid synthesis of aligned zinc oxide nanowires," *Nanotechnology*, vol. 19, no. 25, Article ID 255608, 2008.

[21] J. -S. Huang and C. -F. Lin, "Influences of ZnO sol-gel thin film characteristics on ZnO nanowire arrays prepared at low temperature using all solution-based processing," *Journal of Applied Physics*, vol. 103, no. 1, Article ID 014304, 2008.

[22] M. Wang, C. H. Ye, Y. Zhang, H. X. Wang, X. Y. Zeng, and L. D. Zhang, "Seed-layer controlled synthesis of well-aligned ZnO nanowire arrays via a low temperature aqueous solution method," *Journal of Materials Science: Materials in Electronics*, vol. 19, no. 3, pp. 211–216, 2008.

[23] N. Asakuma, H. Hirashima, H. Imai, T. Fukui, and M. Toki, "Crystallization and reduction of sol-gel-derived zinc oxide films by irradiation with ultraviolet lamp," *Journal of Sol-Gel Science and Technology*, vol. 26, no. 1–3, pp. 181–184, 2003.

[24] Q. Ahsanulhaq, A. Umar, and Y. B. Hahn, "Growth of aligned ZnO nanorods and nanopencils on ZnO/Si in aqueous solution: growth mechanism and structural and optical properties," *Nanotechnology*, vol. 18, no. 11, Article ID 115603, 2007.

[25] B. J. Coppa, R. F. Davis, and R. J. Nemanich, "Gold Schottky contacts on oxygen plasma-treated, n-type ZnO(000$\bar{1}$)," *Applied Physics Letters*, vol. 82, no. 3, pp. 400–402, 2003.

[26] M. Chen, X. Wang, Y. H. Yu et al., "X-ray photoelectron spectroscopy and auger electron spectroscopy studies of Al-doped ZnO films," *Applied Surface Science*, vol. 158, no. 1, pp. 134–140, 2000.

[27] X. Q. Wei, B. Y. Man, M. Liu, C. S. Xue, H. Z. Zhuang, and C. Yang, "Blue luminescent centers and microstructural evaluation by XPS and Raman in ZnO thin films annealed in vacuum, N and O," *Physica B*, vol. 388, no. 1-2, pp. 145–152, 2007.